World Electric Vehicle Journal

MDPI

Article

Optimal EV Charging and PV Siting in Prosumers towards Loss Reduction and Voltage Profile Improvement in Distribution Networks

Christina V. Grammenou, Magdalini Dragatsika and Aggelos S. Bouhouras *

Department of Electrical and Computer Engineering, University of Western Macedonia, University Campus ZEP Kozani, 50100 Kozani, Greece; c.grammenou@uowm.gr (C.V.G.); ece01804@uowm.gr (M.D.)
* Correspondence: abouchouras@uowm.gr; Tel.: +30-246-105-6538

Abstract: In this paper, the problem of simultaneous charging of Electrical Vehicles (EVs) in distribution networks (DNs) is examined in order to depict congestion issues, increased power losses, and voltage constraint violations. To this end, this paper proposes an optimal EV charging schedule in order to allocate the charging of EVs in non-overlapping time slots, aiming to avoid overloading conditions that could stress the DN operation. The problem is structured as a linear optimization problem in GAMS, and the linear Distflow is utilized for the power flow analysis required. The proposed approach is compared to the one where EV charging is not optimally scheduled and each EV is expected to start charging upon its arrival at the residential charging spot. Moreover, the analysis is extended to examine the optimal siting of small-sized residential Photovoltaic (PV) systems in order to provide further relief to the DN. A mixed-integer quadratic optimization model was formed to integrate the PV siting into the optimization problem as an additional optimization variable and is compared to a heuristic-based approach for determining the sites for PV installation. The proposed methodology has been applied in a typical low-voltage (LV) DN as a case study, including real power demand data for the residences and technical characteristics for the EVs. The results indicate that both the DN power losses and the voltage profile are further improved in regard to the heuristic-based approach, and the simultaneously scheduled penetration of EVs and PVs could yield up to a 66.3% power loss reduction.

Keywords: electrical vehicle; mixed-integer quadratic program; distribution network; power quality; penetration; photovoltaic siting

Citation: Grammenou, C.V.; Dragatsika, M.; Bouhouras, A.S. Optimal EV Charging and PV Siting in Prosumers towards Loss Reduction and Voltage Profile Improvement in Distribution Networks. *World Electr. Veh. J.* **2024**, *15*, 462. https://doi.org/10.3390/wevj15100462

Academic Editor: Michael Fowler

Received: 6 September 2024
Revised: 30 September 2024
Accepted: 9 October 2024
Published: 11 October 2024

1. Introduction

In recent years, environmental pollution and the increase in greenhouse gas emissions have become crucial problems for Europe. Combined with the rising prices for gas and oil and the need to reduce CO_2 emissions, the international community has shifted its attention to promoting and encouraging the usage of EVs. In this direction, the EU has signed the "Green Deal" agreement, with the main goal of achieving gas emission reductions of 55% and 100% by 2030 and 2050, respectively [1]. On the one hand, EVs are more eco-friendly and could contribute to reducing carbon emissions, but on the other hand, they are a new type of electric load, which is expected to burden residential installations and the grid. Because of the lack of public charging station infrastructure in many countries, the majority of EVs are expected to be charged in residential installations. Thus, the demand for electricity grows, and the conventional power grid faces new challenges associated with high operational and maintenance costs along with potential violations of its operational parameters. In order to solve these problems, the EU announced Regulation 2022/1854 [2], which mandates that Member States reduce power consumption during peak hours by at least 5%. This decision aims to improve the efficient operation of the DSs,

with an emphasis on minimizing power losses [3]. For example, in Greece, according to the Regulatory Agency of Energy (RAE), energy losses in distribution networks are an important component of the total energy costs incurred by the final consumers. According to the current market design, suppliers bear the cost of the losses, and they incorporate it into the final bills of the consumers. The expected energy losses in the distribution networks are calculated using loss factors, which are calculated by the network operators and approved by RAE. The point is that the increased power losses affect the electricity price and the power supply stability and resilience, which all jeopardize the prosperity of the citizens. According to the published report of the EU Agency for the Cooperation of Energy Regulators, the cost of power losses is either passed directly to consumers through distribution tariffs or is included in the bid price in the energy markets. In both scenarios, the consumers are somehow charged with the cost of power losses [4]. Despite the advantages of EVs for the environment, the uncertain timing of their arrival and the resulting uncontrolled EV charging pose serious problems to the DN, related to power quality, reliability issues, and grid stability. More specifically, uncontrolled EV charging can lead to network congestion, increased power losses, peak demands, and an unbalanced voltage profile. In addition, the uncertainty related to the power production of RES could further worsen this situation if the EV charging fails to coincide with the on-site RES power production. Therefore, several studies have been implemented in order to mitigate these effects. One technique to reduce power losses is the NR scheme [5], which is usually applied to MV networks and aims to determine the optimal topology of the DN under minimum power loss. The basic concerns about NR refer to how frequently the scheme should be applied given the load variations over time. On top of that, if the power losses of the downstream LV DNs of the MV DN are minimized due to EV charging scheduling and PV optimal siting, then the NR application for the MV DN could be proved to be unnecessary in specific time periods. Thus, the idea of smart or optimal charging scheduling for EV charging has gained a lot of attention and become quite popular.

The integration of EVs has been considered in previous studies [6–9], but their charging schedules were not examined. In several studies [7–9], the charging power of the EVs was only used to reform the new load curve in order to strengthen the analysis, while in another study [6], the hosting capacity of the system under a sensitivity analysis regarding the placement of EV charging station at the bus was also examined. In addition, in [10], the authors aimed to determine the optimal size and location of EV charging stations under NR, taking into account their impact on the DN [11]. On the other hand, many studies have examined the charging of EVs combined with the installation of PV in order to address power losses, voltage violations, greenhouse emission reductions, or cost efficiency. For example, the authors in [12] proposed an option to increase the financial benefits for the users of Germany's power grid who use PV self-consumption and apply EV smart charging. The problem was formed as non-linear optimization, and different groups of people and charging strategies (unmanaged, smart unidirectional, and smart bidirectional charging) were utilized in order to minimize the total electricity cost. They placed emphasis only on the revenue for different charging and discharging profiles, without examining the impact of EVs on the grid's total losses or voltage. In addition, the research in [13] reported EVs and EVCSs as controllable loads that can effectively provide grid ancillary services in order to increase the PV hosting capacity. However, EV scheduling and PV siting were not examined. In another study [14], different cases of EV charging were compared with the aim of minimizing the operating cost of the microgrid under study, maximizing the use rate of PV energy, and minimizing the power fluctuation between the main grid and the microgrid; however, PV siting optimization was still not examined.

Some authors have examined the impact of EV charging and penetration of PVs without optimally scheduling EV charging or siting the PV installation. For instance, the work in [15] only presents the DN voltage profile after PV and EV penetration in terms of assessing their impact. Two models were analyzed, and a non-linear optimization problem was formed for the objective function. Moreover, the analysis presented in [16] focused

solely on the impact of EV penetration in DN. A novel dynamic optimization algorithm, based on the Proof of Need (PoN) mechanism, was proposed to efficiently manage EV charging schedules. This approach aimed to mitigate grid power peaks while ensuring user satisfaction and meeting vehicle charging requirements, but it did not account for the simultaneous penetration of PV systems. The authors in [17] investigated how to allocate electricity demand from the power grid for EV owners who have installed distributed solar panels at their homes. A Difference-in-Differences (DID) model was employed to compare consumers with and without EVs, as well as EV owners with and without additional PV systems. The goal was to reduce the average hourly demand from the grid while analyzing the total savings that arise from integrating solar panels with EV charging. Moreover, the authors in [18] proposed the use of metaheuristic algorithms (including particle swarm optimization (PSO), the Salp swarm algorithm (SSA), and the arithmetic optimization algorithm (AOA)) in order to optimally design the structure of an EVFCS connected to a RES and BESS. The RESs were installed to reduce the impact on the grid, while a probabilistic distribution was used for the time of arrival of EVs. The target of this work was the maximization of the profit of the EVFCS determined by its net present value. Generally, metaheuristic algorithms have been extensively applied in problems concerning EV penetration in DNs, but they are prone to local optimum solutions. This is a basic limitation of these approaches. In [19], a metaheuristic algorithm known as the Whale Optimization Technique (WOT) was used to optimize the location and size of EVCS, distribution generators, and shunt capacitors. Its efficiency was evaluated in terms of voltage stability improvement and power loss reduction. Another type of optimization is referred to in [20], known as the stochastic metaheuristic method. This study examined the impact of the uncertainties (arrival and departure of EVs) on a microgrid with RES and EV integration by proposing the Stochastic Monte Carlo Method. In addition to the impact of an uncertain number of EVs, the primary objective of this research was to optimize the system configurations using a metaheuristic algorithm. More specifically, a cost-effective, reliable, and renewable energy system was achieved by employing four metaheuristics algorithms. Finally, the analysis in [21] focused on an optimized charging scheduling algorithm in solar PV-powered grid-connected EV charging stations. A metaheuristic algorithm was used to schedule EV charging by effectively utilizing the PV power under a forecast model of solar power generation with the aim of minimizing charging costs.

In the present study, a two-stage optimization scheme is proposed, including EV smart charging and PV siting. In the first stage, the impact of uncontrolled EV penetration in LV DN is investigated, considering the operational constraints of the DN, in terms of power losses, the voltage profile, and the ampacity level for the lines of the DN. Then, the optimal charging scheduling is formed as a mixed-integer linear optimization problem and, in turn, is solved as a mixed-integer quadratic optimization problem. The results are compared to those under no optimal scheduling to showcase the impact of the smart EV charging on the DN's operational characteristics. In the second stage, the smart EV charging plan is combined with optimal PV siting to further exploit the on-site PV power production towards the DN voltage profile improvement. This is because the PV installation could alleviate grid congestion and increase EV hosting for the DN under study. Aiming to highlight the PV optimal siting approach, we initially examine a heuristic-based approach for the PV siting; this approach indicates the nodes that undergo the most extreme under-voltage issues as critical nodes for PV installation. Then, we come up with the optimal PV siting and compare these two approaches in terms of the voltage profile and power losses for the DN.

Therefore, the main contributions of the present study can be outlined as follows:

- Optimal hourly EV smart charging scheduling in LV DNs is proposed under a mixed-integer linear model aiming at optimizing the voltage profile of the DN.
- Optimal PV siting is integrated into the optimization model to further improve the voltage profile by exploiting the on-site PV power production.

- The impacts of EV and PV penetration, such as increased power losses, congestion, and voltage constraint violations are mitigated due to proper time allocation for EV charging.
- Power peaks in PV production and load demand are also mitigated for the benefit of the DN's operational characteristics.

The rest of the paper is organized as follows. Section 2 presents the mathematical methodology of the heuristic and optimization algorithms for EV charging and PV siting, along with the objective function. Also, the case study and the examined scenarios are analyzed. In Section 3, the results of the study are presented and discussed. Finally, Section 4 concludes the paper.

2. EV Charging Scheduling and PV Siting

2.1. EV Time of Arrival

The proposed methodology examines the impact of EV penetration on power losses, bus voltage, and line loading of a real LV DN. The research is executed in two stages. The first stage includes only EV penetration in the DN, while the second stage integrates the PV installation. One of the most important aspects regarding the impact of EVs on DN is the assessment of EVs' time of arrival. The determination of the EVs' charging scheduling is utilized in two ways, one heuristic and the other under an optimization scheme. Input data such as the time of arrival, EVs' SoC, and the technical characteristics of the EVs, i.e., battery capacity and charger's rate, are taken into account stochastically, as described in the following sections.

Due to the residential profile of the examined DN, it is assumed that the possible EVs' time of arrival ranges from 12:00 to 18:00. The time of arrival depends on the driver's behavior or household characteristics, the mobility data, and the charging rate assumption. The selected interval regarding the EVs' time of arrival has been verified by previous studies [4,22]. In [22], several aspects related to EV charging in DNs are presented. More specifically, the authors in [22] examined the additional power demand by EVs for different days and respective load profiles. The probability concerning the time of arrival was considered different between workdays and weekends. Also, this work presented some data for EV time of arrival depending on the type of EV, charger rate, charging location, and user preferences. Another important parameter that determines the time of arrival is related to demographic characteristics. For example, it differs if someone is unemployed, a full-time or part-time worker, or a homemaker. Based on these data, the analysis in [22] concluded that the time of arrival for EVs varies between 12:00 and 18:00 and follows a nominal distribution. Based on these findings, in this work, we adopt the same approach by applying the normal distribution to define the EVs' time of arrival under different values for the mean value μ and the standard deviation σ.

This time period has been also confirmed by the data analysis conducted by the Adaptive Charging Network Portal [23].

2.2. EV Charging Scheduling

Firstly, the impact of EV penetration is examined without applying any charging schedule. In particular, each EV starts its charging exactly upon arrival and continues until full charging. The arrival time depends on the normal distribution applied, and the range of arrival time is between 12:00 and 18:00, as explained earlier. In order to define the time for the charging of each EV, it is necessary to know the technical characteristics of the EVs, i.e., battery capacity and charger rate, and the SoC when the EV arrives at the respective residence for charging. We define the typical range of SoC at the arrival time of between 20% and 50%, while we consider that each EV can return to its residence once during the day. So, for each of the examined scenarios, the SoC value for an EV upon arrival has been

set randomly to between 20 and 50% under a normal distribution. The time needed for each EV to be fully charged was computed by (1).

$$t_{remainng} = Car_{battery} \times \frac{1 - \frac{SoC}{100}}{Car_{charger}} \quad (1)$$

Based on the resultant time in (1) and the charging rate of the EV, the demand curve of the residence is reformed to consider the additional load caused by EV charging.

Furthermore, as uncontrolled EV charging usually poses challenges for the DN's operation, charging is scheduled using an optimization scheme under linear programming. Initially, the power flow problem is integrated into the optimization model as linear programming in order to avoid the time-consuming non-convex solvers [24] and the drawbacks of metaheuristics algorithms [25]. Subsequently, the linear programming model was converted into a mixed-integer linear program. The reason for this conversion is the utilization of a binary variable $y_{t,i}$ to control the EV charging initialization. This binary variable allows the selection of the appropriate charging time from the given time range for each EV. When the binary variable equals 1, the EV charges, while if the value is 0, then the EV is in idle mode. In addition, it is necessary for each EV to take into account two constraints. As it seems in (2) and (3), the first one is used to ensure that the EV charging time will not exceed the time defined by (1), while the second constraint verifies that the charging will be within the examined time period.

$$\sum_{t=1}^{T} y_{t,i} = t_{remainng} \quad (2)$$

$$t_{arrival\_time} \leq \sum_{t=1}^{T} y_{t,i} + t_{arrival\_time} \leq T \quad (3)$$

The aim of the first stage of this analysis is to optimize the voltage profile of the DN under EV penetration. The case of uncontrolled charging time is compared to the one under the optimal charging schedule in order to showcase the impact of the EV smart charging on the DN's operational characteristics. Thus, the objective function (OF) for both cases is mathematically described in (4):

$$OF = min \sum_{i=1}^{N} (U_a - |U_{t,i}|) \quad (4)$$

The nominal voltage of the slack bus equals 230 V. It should be noted that EV charging is applied on a single-phase LV DN with residential charger stations, and each bus or residential consumer has exactly one EV. The impact of uncontrolled charging along with the optimal charging schedule is assessed in terms of voltage profile improvement, line loading, and power losses for the examined DN. This assessment has been carried out using AC power flow analysis in DigSilent© software 2023 package. The initial optimization scheme was based on a linear formulation for the objective function integrating the linear distflow analysis since the latter yields efficient results with minimal computational overhead, as discussed in [26]. The mathematical modeling of the linear distflow analysis is described in (5)–(7):

$$P_{t,i,j}^{flow} = P_{t,j}^{demand} + (P_{t,j}^{EV} \times y_{t,j}) + \sum_{b}^{N} P_{t,j,b}^{flow}, \forall i < j < b \quad (5)$$

$$Q_{t,i,j}^{flow} = Q_{t,j}^{demand} + (Q_{t,j}^{EV} \times y_{t,j}) + \sum_{b}^{N} Q_{t,j,b}^{flow}, \forall i < j < b \quad (6)$$

$$|U_{t,j}|^2 = \left|U_{t,i,}\right|^2 - 2 \times R_{i,j} \times P_{t,i,j}^{flow} - 2 \times X_{i,j} \times Q_{t,i,j}^{flow}, \ \forall i < j \quad (7)$$

The EVs were considered to inject only active power, i.e., the power factor for all EVs was taken as equal to 1. Also, b represents each downstream bus that connects to the j-th bus, while j is the bus between buses i and b. $\sum_{b}^{N} P_{t,i,b}^{flow}$ is the sum of active power, which

flows through the branch between bus j and downstream buses. The same analysis stands for the $\sum_{b}^{N} Q_{t,j,b}^{flow}$. Based on [27], (7) can be transformed into (8):

$$|U_{t,j}| = |U_{t,i}| - R_{i,j} \times P_{t,i,j}^{flow} - X_{i,j} \times Q_{t,i,j}^{flow}, \forall i < j \quad (8)$$

subject to voltage constraints defined by (9):

$$U^{min} \leq U_{t,i} \leq U^{max} \quad (9)$$

Finally, the aim of the methodology is the improvement of the voltage profile initially formed under the linear expression in (4). Focused on the approach in [28], the objective function is squared to penalize large errors and provide better solutions. Therefore, the mixed-integer linear model is converted to a mixed-integer quadratic model, as presented in (10):

$$OF' = min \sum_{i=1}^{N} \left(U_a - |U_{t,i}|\right)^2 \quad (10)$$

2.3. PV Siting

In the second stage of the proposed methodology, we integrate the PV installation into the optimization model; this is implemented on two levels. In the first level, the impact of EVs' and PVs' penetration is examined simultaneously without applying any charging schedule, as previously performed, or PV siting optimization. Specifically, the installation of PVs is performed using a heuristic approach and PV systems are installed into the so-called critical nodes of the DN. As critical nodes, we consider the nodes with the lowest voltage value magnitude due to EV penetration. It is highly possible that these nodes are the far-end nodes of the branches. In order to decide on the level of criticality for the DN nodes, all nodes are placed in ascending order regarding their voltage magnitude in order to prioritize the selection of nodes with the lowest voltage magnitude. In addition, the frequency of appearance for each node in all 14 examined scenarios, is counted. As a critical node, we consider node j, for which the frequency of appearance f in the 14 scenarios is greater than or equal to 7 (i.e., at least half of the examined scenarios). In total, 7 nodes were present more than 7 times in the examined 14 scenarios. Although the analysis here concerns one day, the same concept for depicting the critical nodes throughout the whole year could also be applied. The flowchart of this approach for selecting the critical nodes is presented in Figure 1.

According to a recent subsidized program in Greece called "PV in Rooftops" for the installation of residential PV systems, the maximum rated power for each residential installation has been set at 10.8 kW. Moreover, according to unofficial data from the Greek DSO, the requests for LV rooftop PV installation usually vary between 3 and 10 kWp and in most cases, the requested PV capacity is no more than 8 kWp. We examined 2 different cases regarding the sizing of the PV systems at the critical nodes, which are presented as follows:

(a) Installation of PVs with nominal power range from 3 kWp to 6 kWp at 7 critical nodes.
(a) Installation of PVs with nominal power range from 5 kWp to 8 kWp at 7 critical nodes.

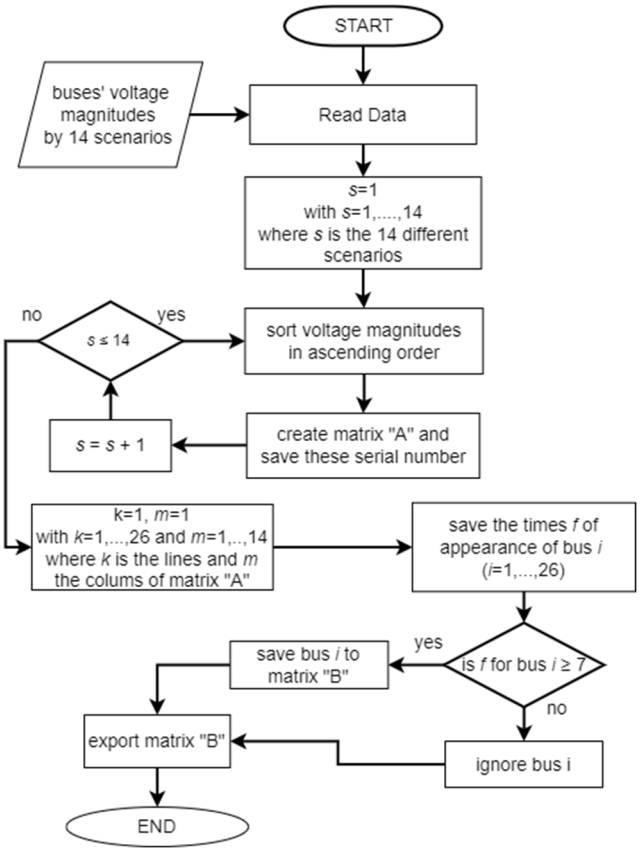

Figure 1. Flowchart of critical node selected.

In addition, at the second level, simultaneous optimal EV charging schedule and PV siting have been examined using a mixed-integer quadratic optimization model. The methodology of this case is similar to the one in Section 2.2 (i.e., optimal EV charging scheduling) with the integration of one more optimization variable into the optimization model regarding the siting of the candidate PV systems under additional constraints. At first, a binary variable $x_{t,i}$ is defined to facilitate PV siting, while the daily PV power production profiles of different-sized PV systems are utilized. Thus, variable $x_{t,i}$ corresponds to each PV at a bus, but each PV system should be installed at exactly one bus and each bus can only host one PV unit, respectively. The sum of $x_{t,i}$ corresponds to the number of PVs that are considered available for installation. Therefore, Equations (5)–(7) are now converted into the ones described in (11)–(13):

$$P_{t,i,j}^{flow} = P_{t,j}^{demand} + (P_{t,j}^{EV} \times y_{t,j}) - (P_{t,j}^{PV} \times x_{t,j}) + \sum_{b}^{N} P_{t,j,b}^{flow}, \forall i < j < b \quad (11)$$

$$Q_{t,i,j}^{flow} = Q_{t,j}^{demand} + (Q_{t,j}^{EV} \times y_{t,j}) - (Q_{t,j}^{PV} \times x_{t,j}) + \sum_{b}^{N} Q_{t,j,b}^{flow}, \forall i < j < b \quad (12)$$

$$|U_{t,j}|^2 = |U_{t,i,}|^2 - 2 \times R_{i,j} \times P_{t,i,j}^{flow} - 2 \times X_{i,j} \times Q_{t,i,j}^{flow}, , \forall i < j \quad (13)$$

In this analysis, it should be noted that the PV systems were considered to inject only active power, i.e., the power factor for all PV systems was taken as equal to 1. In particular, the flowchart in Figure 2 provides a more detailed description of the process.

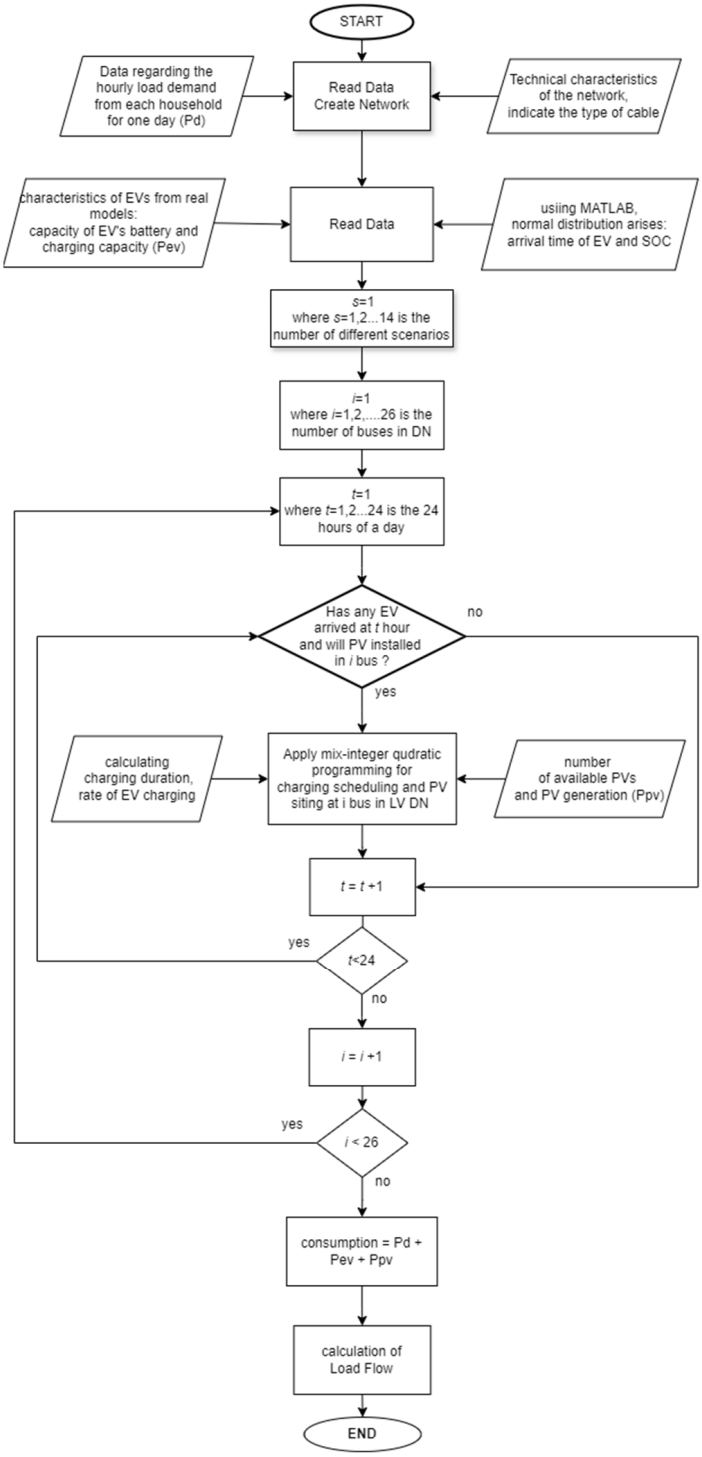

Figure 2. Flowchart of scheduling EV charging and PV siting.

2.4. Case Study

The analysis in this paper aims to examine the penetration of uncontrolled and controlled EV charging, as well as the simultaneous effects of EV charging and PV sitting in an LV DN. This study evaluates the impact on the operational characteristics of the network, i.e., power losses, voltage profile, and loading of lines.

To this end, an LV DN with 26 nodes, i.e., 24 residences, is examined. In Figure 3, the DN layout is presented; the network comprises one MV-to-LV transformer between the first two nodes and several short laterals. The technical characteristics of this, including the line

length and impedance, can be found in [29]. Power flow simulations have been performed in the DigSilent© software 2023 package. Real load demand values for each node–household with a time-step of 1 h spanning a 1 year timeframe were available. The demand curves, i.e., active power demand, of 24 residences are presented in Figure 4 for 24 h.

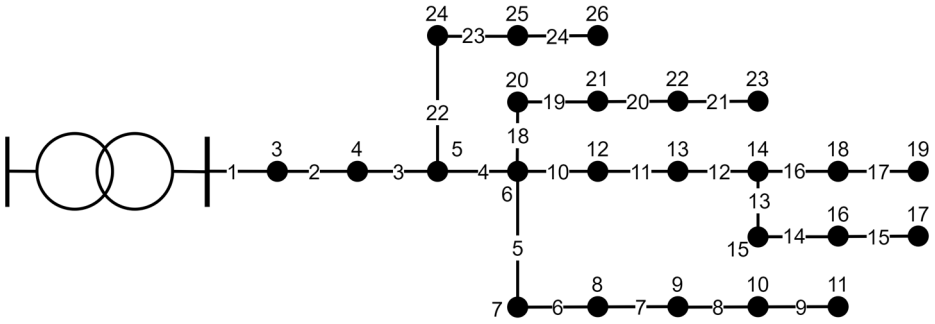

Figure 3. LV network topology.

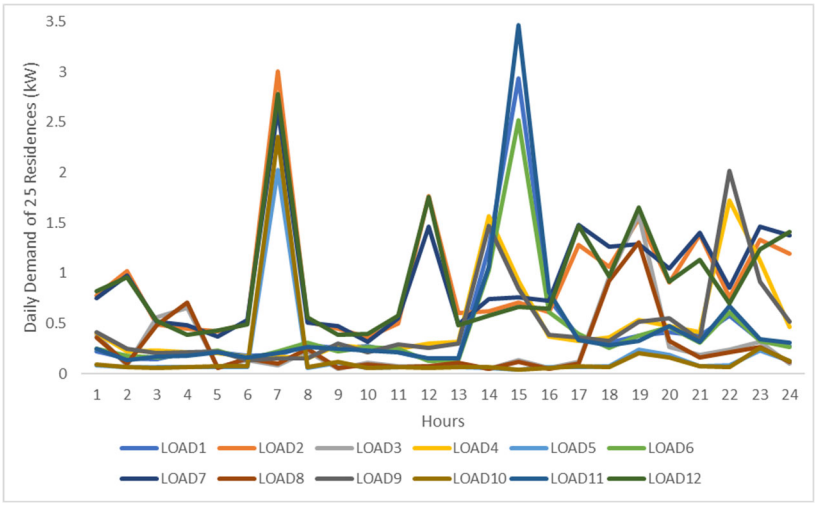

(**a**)

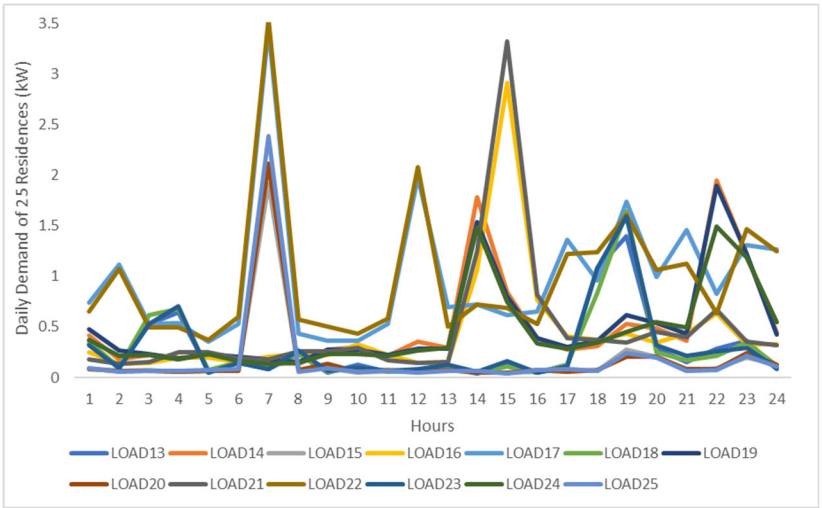

(**b**)

Figure 4. Loads demand: (**a**) loads 1–12; (**b**) loads 13–25.

In the case study of this work, a spring sunny day has been selected with high load demand and PV generation. As mentioned before, each residence has only one EV and the penetration rate of EVs is set at 100%, meaning that all houses are expected to have exactly one EV while each EV returns exactly one time to the charging station. The characteristics of EVs are taken from real EV models and refer to the capacity of the EV's battery and charging rate. In Table 1, the values of these characteristics are presented. Also, the daily PV power production for the examined day is presented in Figure 5 for different-sized PV systems.

Table 1. Characteristics of different EV types.

Types of EVs	Capacity of EV's Battery (kWh)	Charging Capacity (kW)	Number of EVs
1	25	6.6	2
2	36	7.2	1
3	33	7.4	7
4	28	7	6
5	42	7.7	3
6	40	6.6	2
7	100	10	1
8	95	9.6	2
9	75	19.2	1

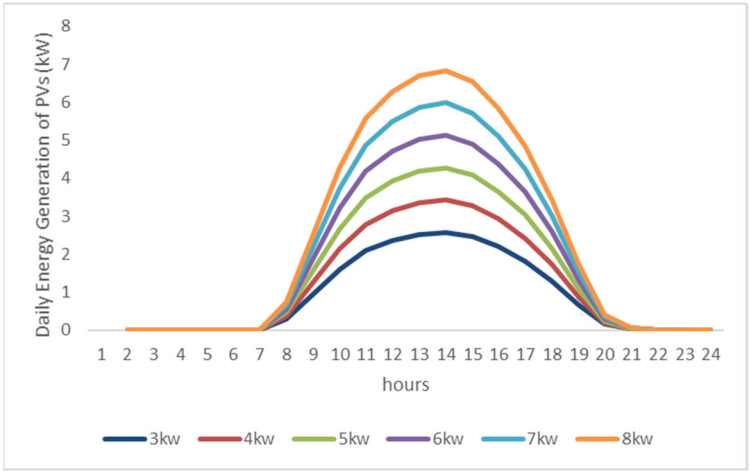

Figure 5. Daily PV generation.

2.5. Examined Scenarios

In the first stage, we aim to evaluate the effect of the time of arrival of EVs on the operational characteristics of the DN. Thus, 14 scenarios were formed with different normal distribution parameters that determine the time of arrival for each EV. As explained previously, in level one, each EV starts its charging exactly upon arrival and continues until full charging without applying any charging schedule. Thus, the differences among these 14 scenarios refer to the different values for the mean value μ and the standard deviation σ. Table 2 analytically shows these values for each scenario. As observed in Table 2, μ ranges between 12:00 and 18:00 (incremental step is 1) to align with the findings presented earlier regarding the expected time of arrival for EVs. The difference between $\sigma = 2$ and $\sigma = 3$ defines the range within which most of the EVs are most likely expected to arrive at the home charging installation. The range $[-\sigma, +\sigma]$ around μ defines a timeframe with a 68% probability of an EV to arrive at its respective residence for charging. For example, in Sc#1, with $\mu = 12$ and $\sigma = 2$, the time of arrival with 68% probability lies between 10:00 and 14:00. Therefore, in Sc#2, with $\mu = 12$ and $\sigma = 3$, the respective range lies between 9:00 and 15:00. In this way, the power curves for all nodes–residences are reshaped and then

the power flow analysis is performed. The simulations in this work concern only BEV but PHEV could also be considered.

Table 2. Simulation scenarios.

Scenarios	Mean Time μ	Standard Deviation σ
Sc#1	12:00	2
Sc#2	12:00	3
Sc#3	13:00	2
Sc#4	13:00	3
Sc#5	14:00	2
Sc#6	14:00	3
Sc#7	15:00	2
Sc#8	15:00	3
Sc#9	16:00	2
Sc#10	16:00	3
Sc#11	17:00	2
Sc#12	17:00	3
Sc#13	18:00	2
Sc#14	18:00	3

On the other hand, in level two, the optimal charging scheduling is applied without the constraint of consecutive charging for an EV. The latter means that the optimization model seeks the optimal number of the required hours to fully charge each EV, but it is not necessary to have the charging in sequential time steps. Using mixed-integer programming, the charging time is selected from the arrival time until 24:00 (the end of the day) in order to minimize the new demand and, in turn, optimize the voltage profile and yield reduced power losses.

In the second stage, the penetration of PVs is further examined. As mentioned in Section 2.3 in the first level, the PVs are installed in 7 critical nodes based on the heuristic approach explained. Two different cases are examined for 14 scenarios subject to different PV systems' sizing. Additionally, in level two, the PV power for the considered systems is the same as level one, but the PV siting is now optimally defined. Specifically, using mixed-integer quadratically programming, the PV siting is determined for the 14 examined scenarios.

As seen before, this study is examined in two stages, involving two different levels for each stage under 14 scenarios. More specifically, these 14 scenarios are applied to 6 cases, due to two ranges for the PV sizing, which are analyzed in more detail in Table 3.

Table 3. Comparison of examined cases.

Cases	First Stage Only EV Penetration	Second Stage EV and PV Penetration	Level One Heuristic EV Charging Scheduling and PV Siting	Level Two Optimal EV Charging Schedule and PV Siting	Power of PV 3–6 kWp	Power of PV 5–8 kWp
Case A	✓	×	✓	×	×	×
Case B	✓	×	✓	×	✓	×
Case C	✓	×	✓	×	×	✓
Case D	×	✓	×	✓	×	×
Case E	×	✓	×	✓	✓	×
Case F	×	✓	×	✓	×	✓

3. Results

In this section, the results derived from the simulations for all examined cases and for all 14 scenarios are presented in order to highlight the impact of optimal EV charging along with optimal PV siting. Thus, the results regarding the daily power losses for the examined DN are presented in Figure 6.

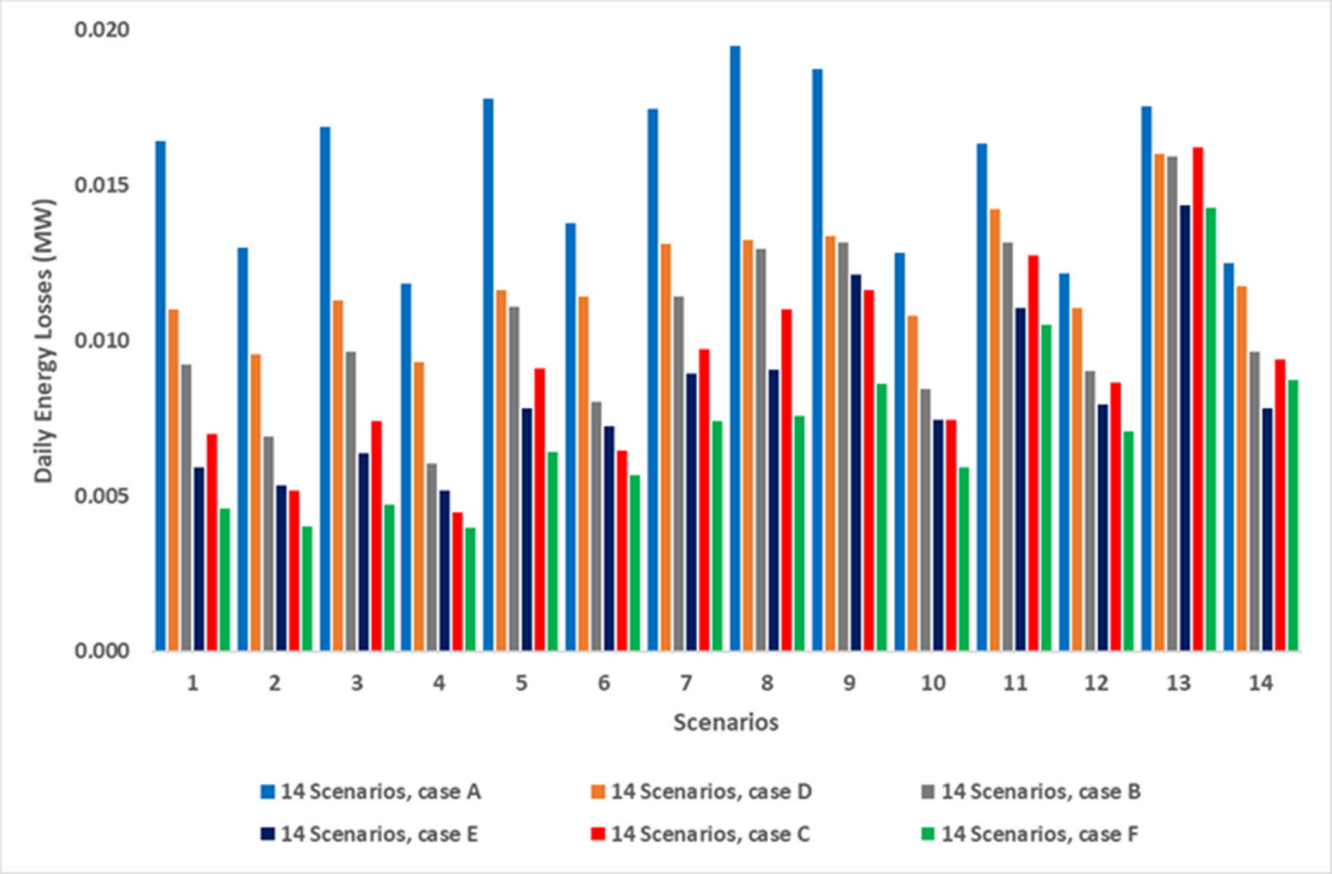

Figure 6. Daily energy losses in 14 scenarios for all 6 cases.

As it seems in Figure 6, in case A (light blue bars), the highest power losses occur as the EVs charge without applying any schedule, while in case D (orange bars), power losses are reduced by up to 22.21% under the optimal EV charging application. Generally, power losses depend on the load profile, the time of arrival, the SoC, and, therefore, the duration of charging. When the PVs are installed, power losses could be mitigated as the on-site PV power production offsets the local power demand. In cases B, C, E, and F, the introduction of PV power systems yields power loss reduction. Comparing cases B and C (grey and red bars) in which PVs are installed at critical nodes with cases E and F (blue and green bars) where optimal PV siting is utilized, we conclude that scenarios with optimal PV siting show higher power loss reduction, at 66.3% and 53.83%, respectively. In contrast, for cases B and C, the reductions in power losses are up to 32.9% and 41.35%. This is more evident when the size of the PVs is larger. All scenarios follow the same trend for the examined cases except for Sc#13 and Sc#14. Specifically, in Sc#13 (μ = 18, σ = 2) and Sc#14 (μ = 18, σ = 3), the time of arrival of most of the EVs varies from 17:00 to 21:00, while PV generation occurs mainly between 7:00 and 20:00, as shown in Figure 5. Therefore, since EV charging does not coincide with PV power production, the DN losses are expected to be higher. Thus, in case F, where the PV power units are larger than in case E, higher losses are observed due to reverse power flow during noon hours.

Furthermore, in all scenarios, the voltage and current profiles of the LV DN have been assessed. However, in this paper, only Sc#5 and Sc#13 are represented because Sc#13 differs from the others, while Sc#5 is representative of all the rest. Additionally, the time of arrival of EVs in Sc#5 is midday, whereas in Sc#13, it is in the afternoon.

Applying the methodology from Section 2, significant differences in the EV charging time slots and for the PV sites are observed under the heuristic approach with the optimization model developed. In Figures 7 and 8, EV charging for Sc#5 and Sc#13 are presented for cases A and D. Specifically, the green color represents uncontrolled EV charging, where the vehicles begin charging immediately upon arrival at the EV station (residence). In contrast, the red color depicts optimal EV charging time slots as a result of the mixed-integer quadratic programming model in this work. Furthermore, in Sc#5 in Figure 7 (m = 12, s = 2), more EVs arrive at midday, but during these hours, residential demand is high. Thus, the optimal algorithm tries to distribute the EV charging throughout the day. However, in Sc#13 in Figure 8 (m = 18, s = 2), many EVs in case D charge in the same time slots as in case A without optimal EV charging. This is because more EVs arrive in the afternoon, leaving insufficient time to charge without charging overlaps.

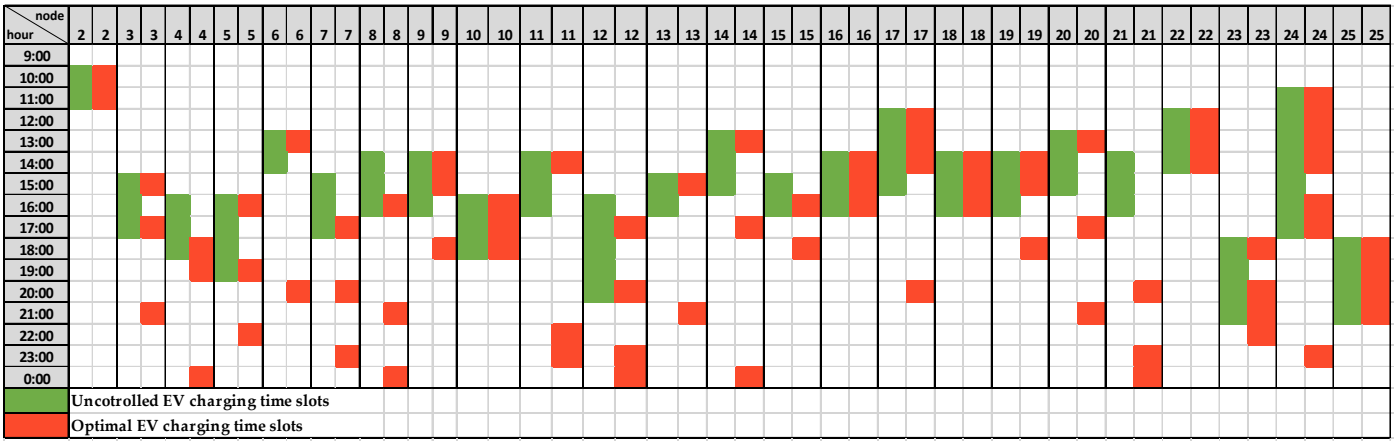

Figure 7. Controlled and uncontrolled EV charging for Sc#5, cases A and D.

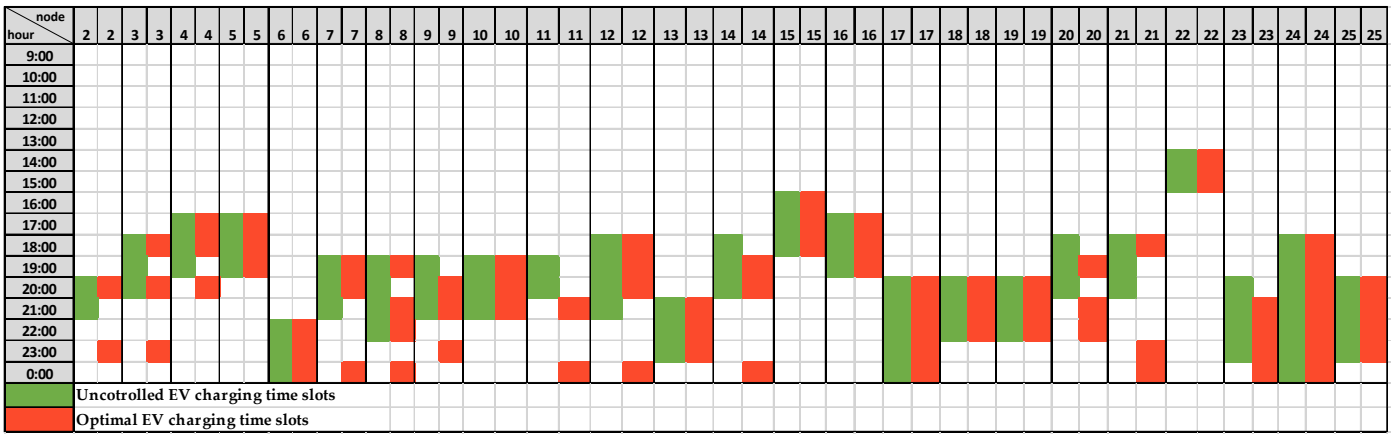

Figure 8. Controlled and uncontrolled EV charging for Sc#13, cases A and D.

In cases B, C, E, and F, the new element refers to the consideration of PV installation in the DN. According to Table 3, in cases B and C, a heuristic algorithm is utilized. Therefore, the PVs were installed in critical nodes 13–19 for all 14 scenarios, as shown in Figure 9. On the other hand, using the optimization model for PV siting, the PV systems are distributed across the DN. For example, in Sc#5, case E, the PVs are installed in nodes 11 and 14–19, while in the same case for Sc#13, the PVs are installed in nodes 3, 4, 9, 14, 15, 22, and 25. As shown in Figure 10, PV siting depends not only on residential and EV demand but also on the sizing of the PVs and on the DN's layout. In case E, PV sizing is lower than in case F.

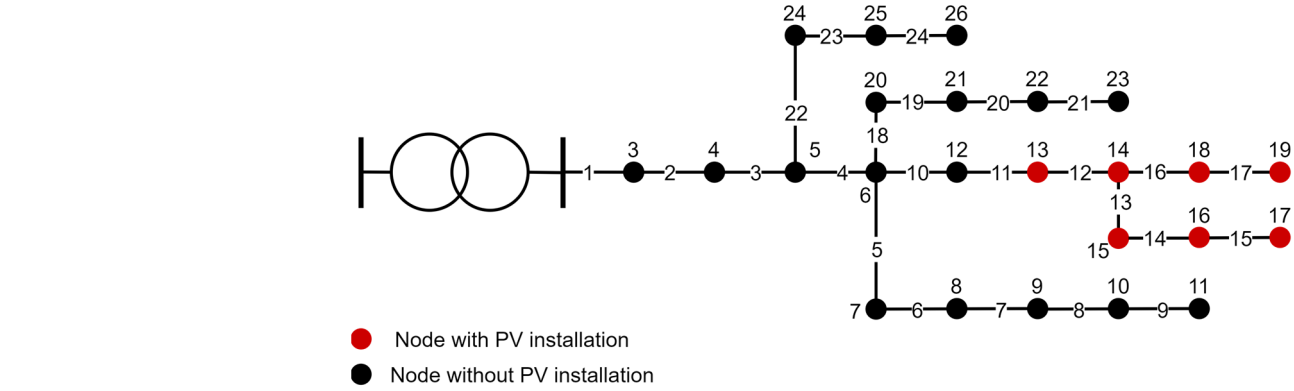

Figure 9. Installation of PVs in critical nodes for 14 scenarios, cases B and C.

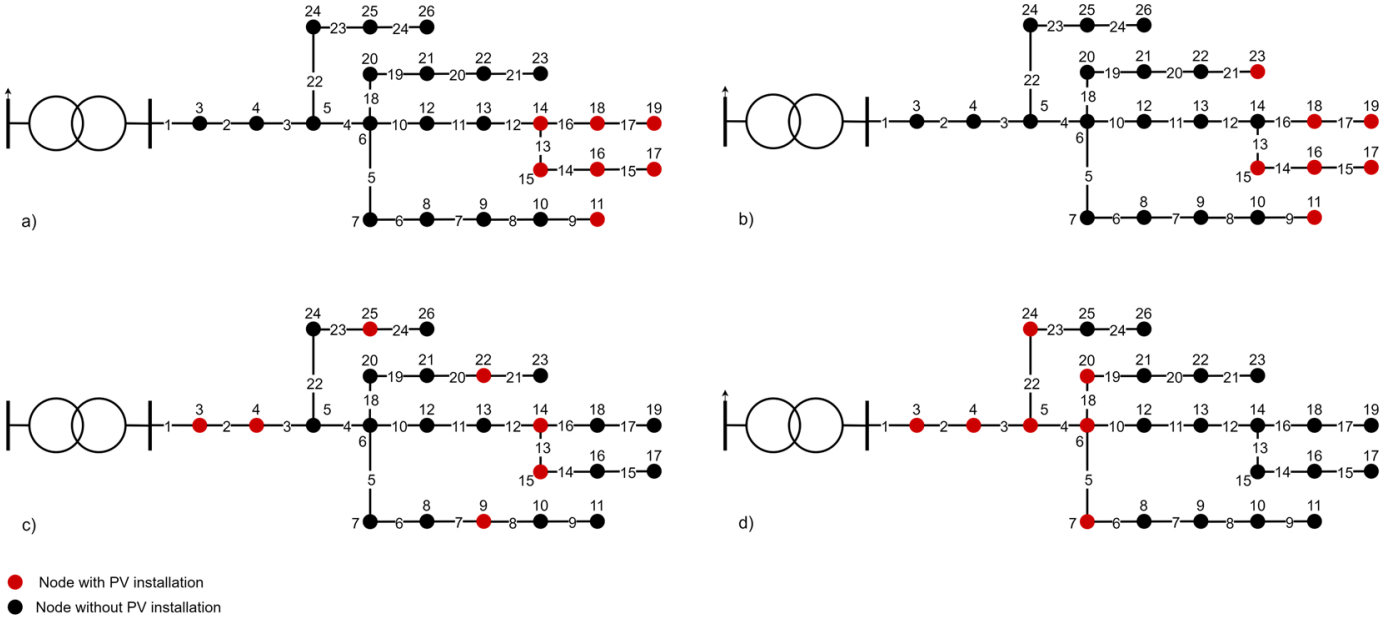

Figure 10. Optimal PV siting: (**a**) Sc#5, case E; (**b**) Sc#5, case F; (**c**) Sc#13, case E; (**d**) Sc#13, case F.

In addition, the voltage profiles during a day for Sc#5 and Sc#13 and for all six examined cases are illustrated in Figures 11 and 12 in boxplots. More specifically, Figure 11 presents the voltage profile of Sc#5 for all six cases. The boxplots in Figure 11a–c represent cases A, B, and C, respectively, which use a heuristic approach either for EV charging or PV siting, while the boxplots in Figure 11d–f represent cases D, E, and F, which use an optimization model. The boxplots in Figure 11a–c present many undervoltage and overvoltage values (i.e., outliers), lying between 220 V and 223 V, compared to the boxplots in Figure 11d–f where no extreme undervoltage or overvoltage values are observed. Moreover, in these boxplots, the voltage follows a consistent pattern, with 50% of the values in all nodes closer to the nominal voltage (except for bus 2).

Subsequently, the voltage profiles throughout the day for Sc#13 for all six cases are represented in Figure 11. The boxplot in Figure 12a, which refers only to EV charging, shows some extreme undervoltage values (i.e., outliers) of 221 V compared to the boxplot in Figure 12d, where no extreme values are observed and 50% of the values in all nodes range from 226 V to 230 V (except for bus 2). In addition, the boxplots in Figure 12b,c present higher overvoltage values of up to 233 V compared to the boxplots in Figure 12e,f where the highest overvoltage value reaches 231 V. Also, in the boxplots for cases E and F, all nodes experience similar boxplots, with 50% of the values in all nodes ranging approximately from 227 V to 230 V (except for bus 2).

Finally, in Figures 13 and 14, color maps for Sc#5 and Sc#13 for all six cases representing line loading are presented. Figure 13 illustrates the current profile regarding Sc#5. As observed, the values of the carrying current in cases A, B, and C with uncontrolled EV charging and PV siting are higher than in cases D, E, and F, which use optimal scheduling for EV charging and PV siting. In particular, in the last three cases, the color maps are almost entirely blue, meaning that line loading is relieved along all lines. Moreover, the highest current values are observed from 12:00 to 17:00 because, in this scenario, the range of arrival times of EVs is from 12:00 to 16:00 and demand is usually high during those hours. Also, PV generation coincides with the arrival times of EVs, reducing line loading.

Similarly, as shown in Figure 14 for Sc#13, the current values in cases A, B, and C, with uncontrolled EV charging and PV siting are higher than in cases D, E, and F, which use optimal scheduling for EV charging and optimal PV siting. Furthermore, the highest current values are presented during the evening hours, specifically from 17:00 to 23:00, as the range of arrival times of EVs is from 12:00 to 16:00. However, despite the PV installation, the voltage profile is not the best since:

(a) PV generation does not coincide with the arrival times of EVs.
(b) The available timeframe for EV charging is very short, thus charging overlaps occur, resulting in peak power demand.

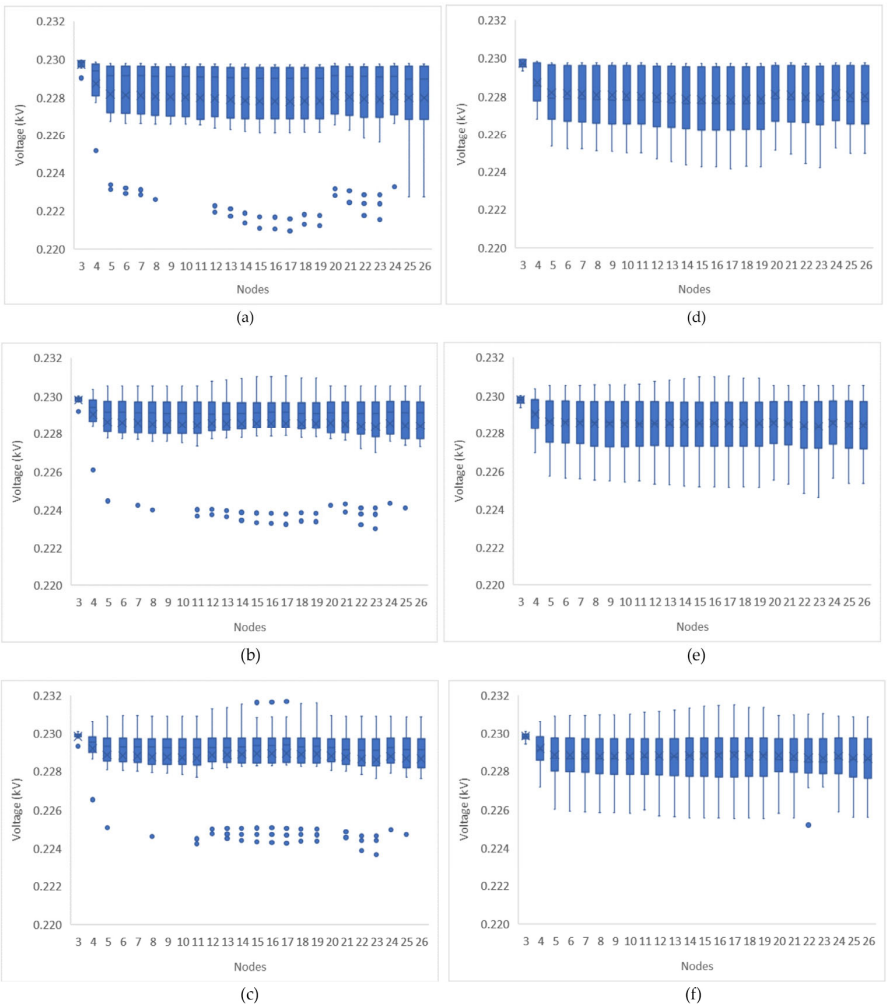

Figure 11. Voltage profile for Sc#5: (**a**) case A, (**b**) case B, (**c**) case C, (**d**) case D, (**e**) case E, and (**f**) case F.

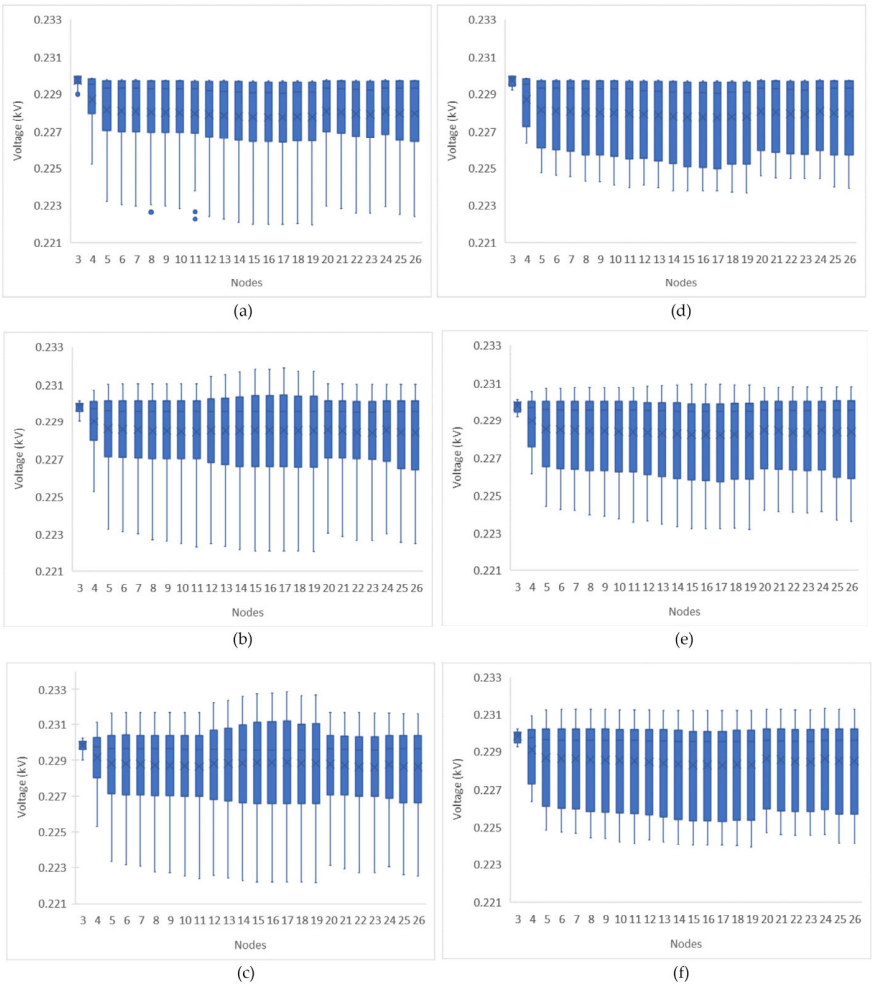

Figure 12. Voltage profile for Sc#13: (**a**) case A, (**b**) case B, (**c**) case C, (**d**) case D, (**e**) case E, and (**f**) case F.

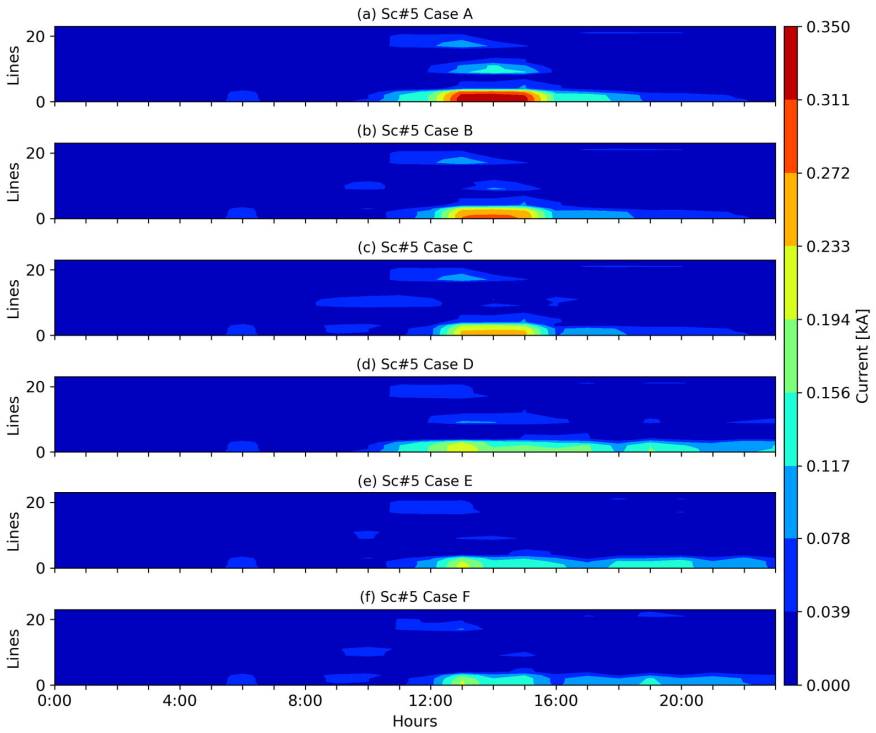

Figure 13. Current profile for Sc#5: (**a**) case A, (**b**) case B, (**c**) case C, (**d**) case D, (**e**) case E, and (**f**) case F.

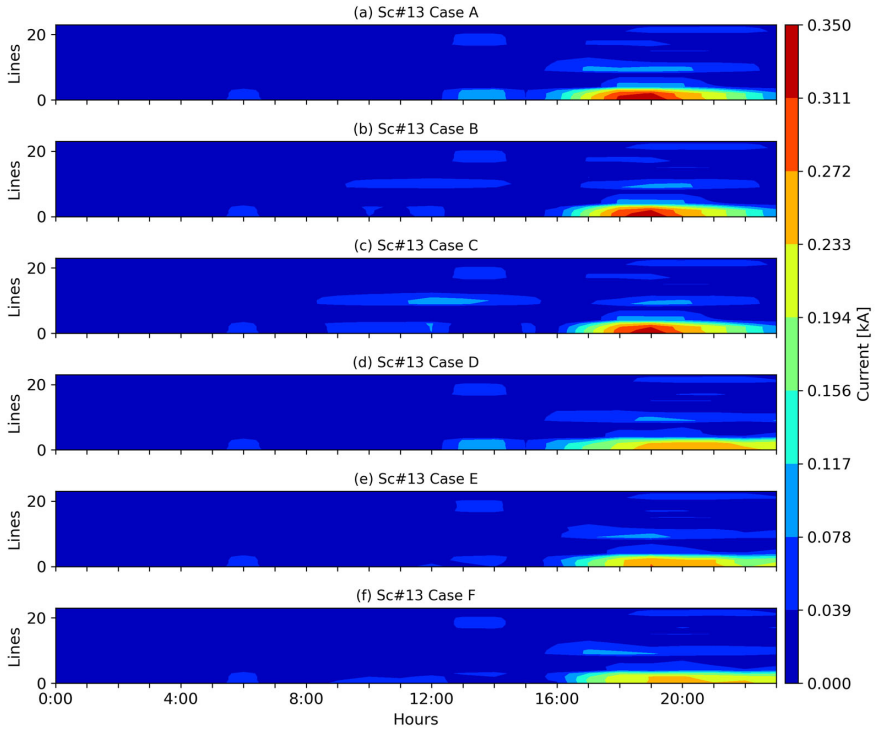

Figure 14. Current profile for Sc#13: (**a**) case A, (**b**) case B, (**c**) case C, (**d**) case D, (**e**) case E, and (**f**) case F.

4. Conclusions

In this paper, the impact of EV and PV penetration in an LV DN under a two-stage, two-level strategy is presented. Issues regarding voltage quality and power losses are addressed by optimally scheduling EV charging and optimally siting the PV systems. Such issues may arise since high PV production during periods of low demand or when PV generation does not coincide with the arrival times of EVs may cause undesirable overvoltage issues. Also, EV charging during periods of high demand could cause severe voltage drops.

Thus, in the first stage of the proposed analysis (three cases examined: A, B, and C), a heuristic approach to EV charging and PV siting is applied. The PVs were installed in seven critical nodes under the criterion of selecting the nodes suffering from the highest undervoltage issues. In the second stage (three cases examined: D, E, and F), an optimization algorithm is proposed for EV charging and PV siting. The proposed charging planning is applied every hour throughout the examined time horizon, considering different PV power units for installation. Moreover, 14 different scenarios regarding the time of arrival for the EVs under a normal distribution are formed.

According to the results of the proposed methodology, which were assessed in an LV DN with real demand data, and by comparing the results of the heuristic approach with those of the optimization algorithm, it appears that:

- Comparing the 14 scenarios of case A under uncontrolled EV charging with the optimal scheduling, a power loss reduction equal to 22.21% is achieved, and the voltage profile is improved as it now ranges from 220 V–230 V instead of 224 V–230 V.
- The employment of PV installation at seven critical nodes using a heuristic approach results in a power loss reduction of 32.9% and 41.36% for the examined scenarios, while a slight voltage increase is observed.
- However, applying optimal PV siting and EV charging scheduling yields a higher loss reduction of between 53.83% and 66.3%, while the voltage profile is further improved since the voltage magnitude varies between 225 V and 231 V.

Author Contributions: Conceptualization, C.V.G., A.S.B.; methodology C.V.G., A.S.B.; software, C.V.G., M.D.; validation, C.V.G., A.S.B., M.D.; formal analysis, C.V.G., M.D.; investigation, C.V.G., A.S.B.; resources, C.V.G., A.S.B.; data curation, C.V.G., M.D.; writing—original draft preparation, C.V.G., A.S.B.; writing—review and editing, C.V.G., A.S.B.; visualization, C.V.G., A.S.B.; supervision, A.S.B. All authors have read and agreed to the published version of the manuscript.

Funding: This research received no external funding.

Data Availability Statement: The original data presented in this study are available on reasonable request from the corresponding author. The data are not publicly available due to privacy.

Conflicts of Interest: The authors declare no conflict of interest.

Nomenclature

Abbreviations	
BESS	Battery Energy Storage Systems
BEV	Battery Electric Vehicles
EVCS	Electric Vehicle Charging Stations
EVFCS	Electric Vehicle Fast-Charging Station
EU	European Union
EV	Electric Vehicle
GAMS	General Algebraic Modeling System
DN	Distribution Network
DS	Distribution System
LV	Low Voltage
MV	Medium Voltage
NR	Network Reconfiguration
SoC	State of Charge
PV	Photovoltaic
PHEV	Plug in Hybrid Electric Vehicles
RES	Renewable Energy Source
Parameters	
$P_{t,i}^{demand}$, $Q_{t,i}^{demand}$	The active and reactive power demand for the residence
$P_{t,i}^{EV}$, $Q_{t,i}^{EV}$	The active and reactive EV power demand
$P_{t,i}^{PV}$, $Q_{t,i}^{PV}$	The active and reactive PV power generation
T	Time period of the scheduling (24 h)
N	Numbers of buses at LV DN
U_a	The nominal voltage of the slack bus (230 V)
$R_{i,j}$, $X_{i,j}$	Resistance and Reactive of line connected from i to bus j
$t_{arrival\_time}$	The EV time of arrival in charge station
$Car_{battery}$	Capacity of EV's battery (kWh)
$Car_{charger}$	Charging capacity (kW)
U^{min}	Lower voltage permissible thresholds
U^{max}	Upper voltage permissible thresholds
Real Variables	
$P_{t,i,j}^{flow}$, $Q_{t,i,j}^{flow}$	The active and reactive powers which flow through the branch between buses i and j.
$U_{t,i}$	The calculated voltage of each bus i at each hour in a day
$t_{remaining}$	Time needed for the EV to fully charge
Sets	
i, j, b	Sets of buses for LV network
t	Sets of hours in a day
Binary Variables	
$y_{t,i}$	Binary variable controls the EV charging initialization (is equal to 1 if EV charges)
$x_{t,i}$	Binary variable is defined to facilitate the PV siting (one PV to each bus)

References

1. Sharma, M.; Sangay, T.; Rangrik, K.; Dorji, N.; Chophel, S. Electric Vehicle Impact Assessment on Distribution Network of Phuentsholing. In Proceedings of the 2022 14th International Conference on Software, Knowledge, Information Management and Applications (SKIMA), Phnom Penh, Cambodia, 2–4 December 2022; pp. 110–113.
2. European Commission. Council Regulation (EU) 2022/1854 of 6 October 2022 on an Emergency Intervention to Address High Energy Prices. 2022. Available online: https://eur-lex.europa.eu (accessed on 21 August 2024).
3. Kothona, D.; Anastasiadis, A.G.; Chrysagis, K.; Christoforidis, G.C.; Bouhouras, A.S. EVs in Distribution Networks—Optimal Scheduling and Real-Time Management. *IEEE Access* **2024**, *12*, 108313–108327. [CrossRef]
4. Kothona, D.; Bouhouras, A.S. A Two-Stage EV Charging Planning and Network Reconfiguration Methodology towards Power Loss Minimization in Low and Medium Voltage Distribution Networks. *Energies* **2022**, *15*, 3808. [CrossRef]
5. Bouhouras, A.S.; Gkaidatzis, P.A.; Labridis, D.P. Network Reconfiguration in Modern Power Distribution Networks. In *Handbook of Optimization in Electric Power Distribution Systems*; Springer: Berlin, Germany, 2020; pp. 219–255.
6. Manan, W.I.A.B.W.A.; Saedi, A.B.; Peeie, M.H.B.; Hanifah, M.S.B.A. Modeling of the Network Reconfiguration Considering Electric Vehicle Charging Load. In Proceedings of the 2021 8th International Conference on Computer and Communication Engineering (ICCCE), Kuala Lumpur, Malaysia, 22–23 June 2021; pp. 82–86.
7. Salkuti, S.R. Network Reconfiguration of Distribution System with Distributed Generation, Shunt Capacitors and Electric Vehicle Charging Stations. In *Next Generation Smart Grids: Modeling, Control and Optimization*; Salkuti, S.R., Ray, P., Eds.; Lecture Notes in Electrical Engineering; Springer: Singapore, 2022; Volume 824, pp. 362–382.
8. Sun, Q.; Yu, Y.; Li, D.; Hu, X. A distribution network reconstruction method with DG and EV based on improved gravitation algorithm. *Syst. Sci. Control. Eng.* **2020**, *9* (Suppl. 2), 6–13.
9. Jangdoost, A.; Keypour, R.; Golmohamadi, H. Optimization of distribution network reconfiguration by a novel RCA integrated with genetic algorithm. *Energy Syst.* **2021**, *12*, 801–833. [CrossRef]
10. Pahlavanhoseini, A.; Sepasian, M.S. Scenario-based planning of fast charging stations considering network reconfiguration using cooperative coevolutionary approach. *J. Energy Storage* **2019**, *23*, 544–557. [CrossRef]
11. Ahmad, F.; Iqbal, A.; Ashraf, I.; Marzband, M.; Khan, I. Optimal location of electric vehicle charging station and its impact on distribution network: A review. *Energy Rep.* **2022**, *8*, 2314–2333. [CrossRef]
12. Ganz, K.; Kern, T.; Hinterstocker, M. Systemic Evaluation of PV Self-Consumption Optimization Using Electric Vehicles. *World Electr. Veh. J.* **2024**, *15*, 98. [CrossRef]
13. Li, X.; Yip, C.; Dong, Z.Y.; Zhang, C.; Wang, B. Hierarchical control on EV charging stations with ancillary service functions for PV hosting capacity maximization in unbalanced distribution networks. *Int. J. Electr. Power Energy Syst.* **2024**, *160*, 110097. [CrossRef]
14. Kumar, S.S.; Iruthayarajan, M.W.; Saravanan, R. Hybrid technique for optimizing charging-discharging behaviour of EVs and demand response for cost-effective PV microgrid system. *J. Energy Storage* **2024**, *96*, 112667. [CrossRef]
15. Soofi, A.F.; Bayani, R.; Manshadi, S.D. Investigating the Impact of Electric Vehicles on the Voltage Profile of Distribution Networks. In Proceedings of the 2022 IEEE Power & Energy Society Innovative Smart Grid Technologies Conference (ISGT), New Orleans, LA, USA, 24–28 April 2022; pp. 1–5.
16. Aoun, A.; Adda, M.; Ilinca, A.; Ghandour, M.; Ibrahim, H. Dynamic Charging Optimization Algorithm for Electric Vehicles to Mitigate Grid Power Peaks. *World Electr. Veh. J.* **2024**, *15*, 324. [CrossRef]
17. Liang, J.; Qiu, Y.; Xing, B. Impacts of the co-adoption of electric vehicles and solar panel systems: Empirical evidence of changes in electricity demand and consumer behaviors from household smart meter data. *Energy Econ.* **2022**, *112*, 106170. [CrossRef]
18. Antarasee, P.; Premrudeepreechacharn, S.; Siritaratiwat, A.; Khunkitti, S. Optimal Design of Electric Vehicle Fast-Charging Station's Structure Using Metaheuristic Algorithms. *Sustainability* **2023**, *15*, 771. [CrossRef]
19. Shweta, M.; Anoop, A. Optimal planning of power distribution system employing electric vehicle charging stations and distributed generators using metaheuristic algorithm. *Electr. Eng.* **2024**, *106*, 1373–1389.
20. Alsharif, A.; Tan, C.W.; Ayop, R.; Al Smin, A.; Ali Ahmed, A.; Kuwil, F.H.; Khaleel, M.M. Impact of Electric Vehicle on Residential Power Distribution Considering Energy Management Strategy and Stochastic Monte Carlo Algorithm. *Energies* **2023**, *16*, 1358. [CrossRef]
21. Titus, F.; Thanikanti, S.B.; Deb, S.; Kumar, N.M. Charge Scheduling Optimization of Plug-In Electric Vehicle in a PV Powered Grid-Connected Charging Station Based on Day-Ahead Solar Energy Forecasting in Australia. *Sustainability* **2022**, *14*, 3498. [CrossRef]
22. Fischer, D.; Harbrecht, A.; Surmann, A.; McKenna, R. Electric vehicles' impacts on residential electric local profiles—A stochastic modelling approach considering socio-economic, behavioural and spatial factors. *Appl. Energy* **2019**, *233–234*, 644–658. [CrossRef]
23. Adaptives Charging Network Research Portal. Available online: https://ev.caltech.edu/index (accessed on 24 February 2021).
24. Morstyn, T.; McCulloch, M.D. Multiclass Energy Management for Peer-to-Peer Energy Trading Driven by Prosumer Preferences. *IEEE Trans. Power Syst.* **2019**, *34*, 4005–4014. [CrossRef]
25. Srilakshmi, E.; Singh, S.P. Energy regulation of EV using MILP for optimal operation of incentive-based prosumer microgrid with uncertainty modelling. *Int. J. Electr. Power Energy Syst.* **2022**, *134*, 107353. [CrossRef]
26. Nakiganda, A.M.; Dehghan, S.; Aristidou, P. Comparison of AC Optimal Power Flow Methods in Low-Voltage Distribution Networks. In Proceedings of the 2021 IEEE PES Innovative Smart Grid Technologies Europe (ISGT Europe), Espoo, Finland, 18–21 October 2021; pp. 1–5.

27. Turitsyn, K.; Sulc, P.; Backhaus, S.; Chertkov, M. Local Control of Reactive Power by Distributed Photovoltaic Generators. In Proceedings of the 2010 First IEEE International Conference on Smart Grid Communications, Gaithersburg, MD, USA, 4–6 October 2010; pp. 79–84.
28. Kelepouris, N.S.; Nousdilis, A.I.; Bouhouras, A.S.; Christoforidis, G.C. Optimal scheduling of prosumer's battery storage and flexible loads for distribution network support. *IET Gener. Transm. Distrib.* **2023**, *17*, 1491–1508. [CrossRef]
29. Kryonidis, G.; Kontis, E.; Chrysochos, A.; Demoulias, C.S.; Papagiannis, G. A coordinated droop control strategy for overvoltage mitigation in active distribution networks. *IEEE Trans. Smart Grid* **2017**, *9*, 5260–5270. [CrossRef]